

## Supplementary Information for

Oligodendrocyte precursor survival and differentiation requires chromatin remodeling by Chd7 and Chd8

Corentine Marie<sup>1</sup>, Adrien Clavairoly<sup>1</sup>, Magali Frah<sup>1</sup>, Hatem Hmidan<sup>1</sup>, Jun Yan<sup>3</sup>, Chuntao Zhao<sup>2</sup>, Juliette Van Steenwinckel<sup>3</sup>, Romain Daveau<sup>1</sup>, Bernard Zalc<sup>1</sup>, Bassem Hassan<sup>1</sup>, Jean-Léon Thomas<sup>1,4</sup>, Pierre Gressens<sup>3</sup>, Philippe Ravassard<sup>1</sup>, Ivan Moszer<sup>1</sup>, Donna M. Martin<sup>5</sup>, Q. Richard Lu<sup>2</sup>, and Carlos Parras<sup>1</sup>

Correspondence should be addressed to C.P. ([carlos.parras@upmc.fr](mailto:carlos.parras@upmc.fr))

### **This PDF file includes:**

Supplementary Information Text  
Figs. S1 to S15  
Tables S1 to S2  
Dataset S1 to S2  
Supplemental references

**Supplementary Information Text**  
**SUPPLEMENTAL MATERIAL & METHODS**

**Materials**

**KEY RESOURCES TABLE**

<b>REAGENT or RESOURCE</b>	<b>SOURCE</b>	<b>IDENTIFIER</b>
<b>Chemicals, Peptides, and Recombinant Proteins</b>		
Pifithrin- $\alpha$ (PFT)	Sigma	P4359
Tamoxifen	Sigma	T5648
lysolecithin (LPC)	Sigma	L4129
5-Bromo-2'-deoxyuridine (BrdU)	Sigma	16880
<b>Critical Commercial Assays</b>		
Neural tissue dissociation kit (T)	Miltenyi biotech	130-093-231
Nextera DNA sample kit	Illumina	15028212
iDeal CHIP-seq kit for Transcription Factor	Diagenode	C01010055
<b>Deposited Data</b>		
RNA-seq data	This paper	GSE116600
Chd7 CHIP data MOUSE OPC	This paper	GSE116599
Chd8 CHIP data MOUSE OPC	This paper	GSE116599
ATAC-seq data	This paper	GSE116598
<b>Experimental Models: Organisms/Strains</b>		
Mice CD1 wt	Janvier	
Chd7 <sup>Flox/Flox</sup>	Donna M. Martin	(1, 2)
PDGFR $\alpha$ -CreERT	Dwight Bergles	(Kang et al., 2010)
ROSA26R <sup>stop-floxed-YFP</sup>	Jackson lab	(3)
<b>Oligonucleotides</b>		
RTqPCR primers see Table S2	Various papers (See Table S2)	N/A
<b>Software and Algorithms</b>		
Zen	N/A	<a href="https://www.zeiss.com/">https://www.zeiss.com/</a>
ImageJ	N/A	<a href="https://imagej.nih.gov/ij/">https://imagej.nih.gov/ij/</a>
Genomatix	N/A	<a href="https://www.genomatix.de">https://www.genomatix.de</a>
Pathway Studio	N/A	<a href="http://www.pathwaystudio.com/">http://www.pathwaystudio.com/</a>
TopHat59	N/A	<a href="https://ccb.jhu.edu/software/tophat/index.shtml">https://ccb.jhu.edu/software/tophat/index.shtml</a>
Bowtie2	(Langmead and Salzberg, 2012)	<a href="http://bowtie-bio.sourceforge.net/bowtie2/index.shtml">http://bowtie-bio.sourceforge.net/bowtie2/index.shtml</a>
Samtools	(Li et al., 2009)	<a href="http://samtools.sourceforge.net/">http://samtools.sourceforge.net/</a>
MACS2	(Zhang et al., 2008)	<a href="https://github.com/taoliu/MACS/">https://github.com/taoliu/MACS/</a>
IGV	(James et al., 2011)	<a href="http://software.broadinstitute.org/software/igv/home">http://software.broadinstitute.org/software/igv/home</a>

ANTIBODIES	SOURCE	DILUTION	IDENTIFIER
Mouse anti-Ascl1/Mash1	BD Biosciences	1/200	Clone 24B72D11.1
Mouse anti-APC (CC1)	Millipore	1/200	Cat#OP80 RRID:AB_213434
Rabbit anti-APC	Santa Cruz Biotechnology	1/200	Cat#sc-896 RRID:AB_2057493
Mouse anti-beta-III-tubulin	BABCO	1/1000	MMS-435P
Rat anti-BrdU	Oxford biotechnology	1/20	Cat#OBT0030S
Rabbit anti-Casp3	R&D systems	1/250	Cat#AF835, RRID:AB_2243952
Rabbit anti-Chd7	Cell signaling	1/1000	Cat#6505S RRID:AB_11220431
Sheep anti-Chd7	R and D Systems	1/100	Cat#AF350 RRID:AB_10994180
Rabbit anti-Chd8	Bethyl	1/1000	Cat#A301-224A RRID:AB_890578
Mouse anti-CNP	Millipore	1/100	Cat#MAB326R RRID:AB_2082608
Rabbit anti-Itpr2	Millipore	1/500	Cat#AB3000
Chicken anti-GFAP	Aves labs	1/1000	Cat#GFAP
Chicken anti-GFP	Aves labs	1/2000	Cat#GFP-1020, RRID:AB_10000240
Rabbit anti-Iba1	WAKO Chemicals GMBH	1/500	Cat#019-191741
Rat anti-Ki67	Leica	1/500	Cat#M-7249
Mouse anti-MCM2	BD biosciences	1/500	Cat#610701 RRID:AB_398024
Mouse anti-MOG	Developmental Studies Hybridoma Bank	1/5	Clone AA3
Mouse anti-Nkx2.2	Developmental Studies Hybridoma Bank	1/4	clone 74.5A5
Rat anti-PDGFR $\alpha$	BD Bioscience	1/400	Cat#558774 RRID:AB_397117
Mouse anti-Olig1	NeuroMab	1/500	Cat#75-180
Mouse anti-Olig2	Millipore	1/500	Cat#MABN50, RRID:AB_10807410
Rabbit anti-p53	Leica	1/500	Cat#P53-CM5P-L

## Methods

### *Mice*

*ROSA26R<sup>stop-floxed-YFP</sup>* mouse line were crossed with *PDGFR $\alpha$ -CreER<sup>T</sup>*; *Chd7<sup>Flox/Flox</sup>* to generated iKO mice with YFP reporter. The mouse strains used in this study were generated and housed (six or less animals per cage) in a vivarium with a 12-h light/dark cycle. Wild-type Swiss mice were obtained from Janvier Labs.

### *Tamoxifen administration*

Alternatively, tamoxifen (Sigma, T5648) was dissolved in corn oil (Sigma, C-8267) and injected subcutaneously at 20mg/ml concentration at postnatal stages P7 (30 $\mu$ l) in *Ctrl* and *Chd7iKO* animals. Brains were then collected at P20.

### ***BrdU administration***

5-Bromo-2'-deoxyuridine (BrdU, Sigma, 16880) was dissolved in NaCl at 10 mg/ml and injected intraperitoneally at 10  $\mu$ l/g at postnatal stages P7 in tamoxifen-induced *Ctrl* and *Chd7iKO* animals, 1 hour before perfusion.

### ***Demyelinating lesions***

Before surgery, adult (2-3months) mice were weighted and anesthetized by intraperitoneal injection of mixture of ketamine (0.1 mg/g) and xylazine (0.01 mg/g). Focal demyelinating lesions were induced by stereotaxic injection of 1 $\mu$ l of lysolecithin solution (LPC, Sigma, L4129, 1% in 0.9%NaCl) into the corpus callosum (CC; at coordinates: 1 mm lateral, 1.3 mm rostral to bregma, 1.7 mm deep to brain surface) using a glass-capillary connected to a 10 $\mu$ l Hamilton syringe. Animals were left to recover in a warm chamber before being returned into their housing cages. Brains were collected 2 or 4 days after lesions (2-4 dpi).

### ***Tissue processing***

Postnatal mice were anesthetized and perfused with 15 ml (for P7) and 25ml (for older animals) 2% paraformaldehyde (EMS, 15714). Brains were dissected, dehydrated in 20% sucrose at 4°C, embedded in OCT for freezing and cryosectioned at 14  $\mu$ m.

### ***Immunohistochemistry***

Postnatal mouse brain cryosections (14- $\mu$ m thick) were permeabilized and blocked in blocking buffer (0.05% Triton X-100 and 10% normal goat serum in PBS) for 1 hour and overlaid with primary antibodies overnight at 4°C. Antibody details are provided in supplemental material. After washing with 0.05% Triton X-100 in PBS, sections were incubated with secondary antibodies conjugated to Alexa488, Alexa594 or Alexa647 (Thermo, 1:1,000) and DAPI for 1 hour at room temperature, washed in PBS and mounted with Fluoromount-G (SouthernBiotech). For BrdU immunostaining, after normal staining for other required antibodies, sections were post-fixed with 4% PFA at

RT for 5 minutes before pretreatment with 2N HCl in PBS at 37°C for 30min, and normal immunostaining protocol with anti-BrdU antibody.

For cells, coverslips were fixed in 4% paraformaldehyde for 10 minutes at room temperature and washed in PBS. They were blocked for 1h at room temperature in blocking buffer (0.05% Triton X-100 and 10% normal goat serum in PBS) and overlaid with primary antibodies for 30min at room temperature. After washing with 0.05% Triton X-100 in PBS, cells were incubated with secondary antibodies conjugated to Alexa488, Alexa594 or Alexa647 (Thermo, 1:1,000) and DAPI for 30min at room temperature, washed in PBS and mounted with Fluoromount-G (SouthernBiotech).

Pictures of were taken with Zeiss microscope using Apotome system optical sectioning and deconvolution. Z-stack was used. Zen and ImageJ software packages were used to treat pictures and perform cell quantifications. For cells on coverslips, pictures were taken using CellInsight (Thermo Scientific).

### ***MACSorted OPC culture***

To control sorted cell population, cells were put on coverslips coated with poly-ornithine (Sigma, P4957) and cultured for a couple of hours in medium composed of DMEM high glucose GlutaMAX™ Supplement (ThermoFisher, 61965-026), B27 supplement (ThermoFisher, 17502048), EGF (Peprotech, AF-100-15, 20ng/ml), FGF (Peprotech, 100-18B, 10ng/ml) and PDGF (Peprotech, 100-13A, 10ng/ml) at 37°C. They were then fixed in 4% paraformaldehyde (PFA, diluted from 32% PFA, EMS, 15714) for 10 minutes, before processing to immunostaining.

### ***In vitro lentiviral transduction***

NSCs from *WT*, *ROSA26R<sup>stop-floxed-YFP</sup>* and *Chd7<sup>Flox/+</sup>; ROSA26R<sup>stop-floxed-YFP</sup>* brains were dissociated and put in neurosphere medium enriched in EGF (20ng/ml; Peprotech; AF-100-15) and FGF (10ng/ml; Peprotech; 100-18B). Two days prior to transduction, cells were put in proliferation medium containing EGF, FGF and PDGF-AA (10ng/ml; Peprotech, 100-13A). Cells were then plated on coverslips coated with Poly-L-ornithine

(Sigma, P4957) and transduced using lentiviral particles expressing the Cre recombinase and either a shRNA against Chd8 (GCAGTTACACTGACGTCTACA) or a scramble shRNA (TCGTCATAGCGTGCATAGGTTCAAGAGACCTATGCACGCTATGACGA). One day after transduction, cells were put in differentiation medium without growth factors and after 3 or 6 days of differentiation, fixed with 4% formaldehyde.

### ***ChIP-Seq and data analysis***

ChIP-seq assays were performed using iDeal ChIP-seq kit for Transcription Factors (Diagenode, C01010055). Briefly, 4 million fresh sorted OPCs were fixed in 1% formaldehyde (EMS, 15714) for 10 min at room temperature. Lysate were sonicated with a Bioruptor Pico sonicator (Diagenode, total time 8 min) and 4µg of antibodies were added to chromatin and incubated at 4°C overnight. Rabbit anti-Chd7 (Cell signaling, 6505) and anti-Chd8 (Bethyl, A301-224A) antibodies were used for immunoprecipitation experiments. Chromatin-protein complexes were immunoprecipitated with protein A/G magnetic beads and washed sequentially. Input and Mock (Rabbit IgG) ChIP were used as controls in each individual experiments.

The ChIP-seq libraries were prepared using TruSeq ChIP library preparation kit (Illumina ip-202-1012), sequenced with Illumina HiSeq 2500 platform and mapped using bowtie2 onto mm10. Low-quality reads were filtered-out with SAMtools and PCR-derived duplicates removed by using PICARD MarkDuplicates. Peak calling was performed using MACS (Model-based Analysis of ChIP-Seq) (<http://liulab.dfci.harvard.edu/MACS>) with options: keep-dup all, nolambda, broad, nomodel, extsize 75 -q 0.01 and filtered according to the following criteria: (i) length>=100bp and (ii) p-value<=5%. Two and one separate experiments were done for Chd7 and Chd8, respectively.

Representation of the data, overlapping, region annotation and correlations were done using Genomatix ([www.genomatix.de](http://www.genomatix.de)) and IGV browser (<https://software.broadinstitute.org/software/igv/>). GO analysis were done using Pathway Studio (Elsevier, [www.pathwaystudio.com/](http://www.pathwaystudio.com/)). “Promoters” correspond to

regions 1000bp upstream of transcription start site (TSS) and 10bp downstream of TSS (Genomatix). “Enhancers” correspond to the regions commonly bound by Sox10 and Olig2 (4, 5). Gene expression profiles have been analyzed from OL stage specific transcriptome and single-cell analysis (6, 7).

#### ***RNA extraction and RT-qPCR.***

RNAs were extracted from at least 10<sup>5</sup> MACsorted O4<sup>+</sup>-cells from P7 *Chd7iKO* mice and their control littermates, using Nucleospin RNA kit (Macherey-Nagel, 740955). cDNAs were generated with SuperScript cDNA Synthesis Kit (Invitrogen, 18080051). RT-qPCR were performed using LightCycler<sup>®</sup> 96 real-time PCR system (Roche) and LightCycler<sup>®</sup> 480 SYBR Green I Master mix (Roche, 4707516001 ). Primers details are given in SI Appendix, Table S2. *β-actin* was used for normalization.

#### ***RNA-seq and data analysis***

RNA-seq libraries from *control* (*n*=7) and *Chd7iKO* (*n*=5) OPCs were prepared using TruSeq Stranded mRNA (Illumina 20020594) and sequenced with Illumina HiSeq 2500 platform. RNA-seq reads were aligned onto the mm10 reference transcriptome using bowtie and quantified using eXpress. The edgeR R-package was used to perform both data normalization and differential expression analyses. In all differential expression tests, genes were considered regulated when p-value < 0.05 and Fold change > 1.2. Heatmap of gene expression was generated using R language (<http://www.r-project.org>). GO analysis of genes repressed and increased in *Chd7iKO* mutants was performed using Pathway Studio (Elsevier, [www.pathwaystudio.com/](http://www.pathwaystudio.com/)).

#### ***ATAC-seq and data analysis***

10<sup>5</sup> OPCs from control and *Chd7iKO* P7 mice were purified and lysate before ATAC-seq reaction, which was done as described before (8). Libraries were done using Nextera DNA sample kit (Illumina, 15028212) and sequenced with Illumina HiSeq 2500 platform.

Reads from 5 controls and 5 *Chd7iKO* were uniquely mapped onto mm10 with bowtie2. Low-quality, mitochondria- and PCR-derived reads were all removed and peaks were called by using MACS. Regarding ChIP-seq data, only significant peaks  $\geq 100$ bp were considered for downstream analyses.

### ***Statistical Analysis***

Statistical parameters including the exact value of n, the definition of center, dispersion and precision measures (mean  $\pm$  SEM) and statistical significance are reported in the Figures, Figure Legends and SI Appendix, Dataset S2. 'n' represent the number of animals in histological studies and number of samples in RNA-seq, ChIP-seq and ATAC-seq studies. Data distribution was assumed to be normal, but this was not formally tested. Statistical significance was determined using two-tailed Student's t tests. One-way ANOVA test was performed for multiple comparisons or pairwise comparisons following Turkey's ranking tests when comparing multiple groups. Data are judged to be statistically significant when  $p < 0.05$ . In figures, asterisks denote statistical significance as calculated by Student's t test (\*,  $p < 0.05$ ; \*\*,  $p < 0.01$ ; \*\*\*,  $p < 0.001$ ). No statistical methods were used to predetermine sample sizes, but our sample sizes are similar to those generally employed in the field to balance experimental robustness with the 3R rule for animal experimentation. Quantifications were performed from at least three independent experiments. No randomization was used to collect all the data, but they were quantified blindly. Statistical analysis was performed in Prism software.

### ***Data Resources***

Raw data files have been deposited in the NCBI Gene Expression Omnibus under accession number GEO: GSE116601

### ***Contact for Reagent and Resource Sharing***

Further information and requests for reagents may be directed to, and will be fulfilled by the corresponding author Carlos Parras ([carlos.parras@upmc.fr](mailto:carlos.parras@upmc.fr)).



# SUPPLEMENTAL FIGURES

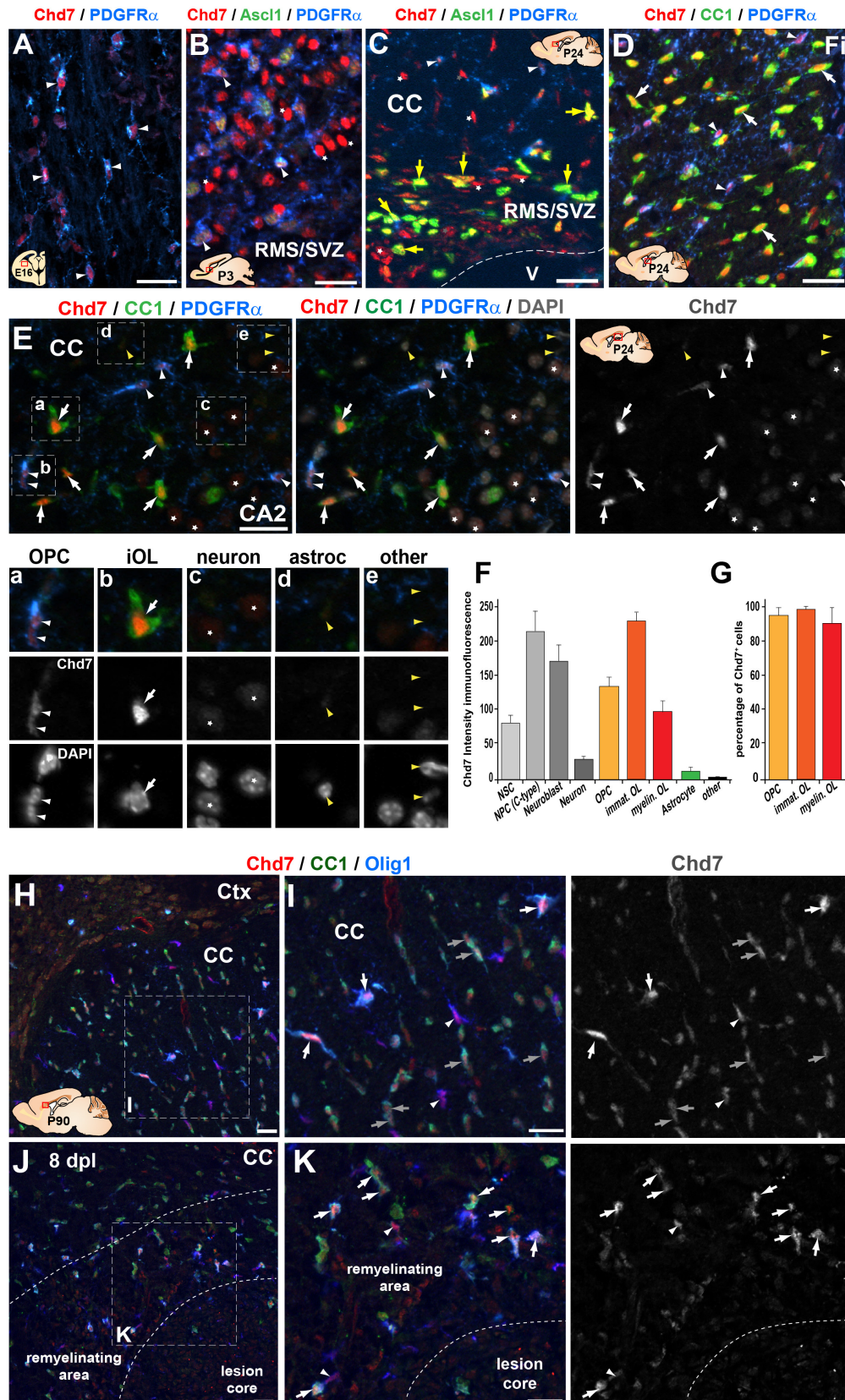


**Fig. S1. (related to Figure 1)**

A – Immunostaining of Chd7 and PDGFR $\alpha$  in the ventral telencephalon of E16.5 WT mouse. Arrow heads represent PDGFR $\alpha$ <sup>+</sup> OPCs expressing Chd7. Scale bar: 20  $\mu$ m.

B – Immunostaining of Chd7, Ascl1 and PDGFR $\alpha$  in the SVZ of P3 WT mouse. Arrow heads represent PDGFR $\alpha$ <sup>+</sup> OPCs expressing Chd7 and Ascl1 and stars represent neuroblasts. Scale bar: 20  $\mu$ m.

C – Immunostaining of Chd7, Ascl1 and PDGFR $\alpha$  in the corpus callosum and SVZ of P24 WT mouse. White arrow heads represent PDGFR $\alpha$ <sup>+</sup> OPCs expressing Chd7, yellow arrows represent Ascl1<sup>+</sup> progenitors expressing Chd7 and stars represent neuroblasts. Scale bar: 20  $\mu$ m.

D – Immunostaining of Chd7, PDGFR $\alpha$  and CC1 in the fimbria of P24 WT mouse. Arrow heads represent PDGFR $\alpha$ <sup>+</sup> OPCs expressing Chd7, arrows represent CC1<sup>+</sup> OLs expressing Chd7. Scale bar: 20  $\mu$ m.

E – Immunostaining of Chd7, PDGFR $\alpha$  and CC1 in the corpus callosum of P24 WT mouse. White arrow heads represent PDGFR $\alpha$ <sup>+</sup> OPCs expressing Chd7, white arrows represent CC1<sup>+</sup> OLs expressing Chd7, stars represent neurons, and yellow arrow heads represent astrocytes and other cell-types. a, b, c, d and e are higher magnification of the inset in E. Scale bar: 20  $\mu$ m.

F – Quantification of Chd7 intensity of immunofluorescence in different cell-types at P24. Data are presented as mean  $\pm$  s.e.m.

G – Quantification of Chd7<sup>+</sup> cells as a percentage of total OPCs, iOLs and mOLs in P24 mice.

H – Immunostaining of Chd7, Olig1 and CC1 in the corpus callosum of P90 adult WT mouse. Scale bar: 20  $\mu$ m.

I – Higher magnification of the inset in H. White arrow heads represent Olig1<sup>+</sup> OPCs, white arrows represent Olig1<sup>High</sup>-CC1<sup>High</sup> iOLs and grey arrows represent Olig1<sup>Low</sup>-CC1<sup>Low</sup> mOLs. Scale bar: 20  $\mu$ m.

J – Immunostaining of Chd7, Olig1 and CC1 in the remyelination area at 8 days post-lesion (8dpi) in the corpus callosum of P90 adult WT mouse. Scale bar: 20  $\mu$ m.

K – Higher magnification of the inset in J. White arrow heads represent Olig1<sup>+</sup> OPCs and white arrows represent Olig1<sup>High</sup>-CC1<sup>High</sup> iOLs. Scale bar: 20  $\mu$ m.

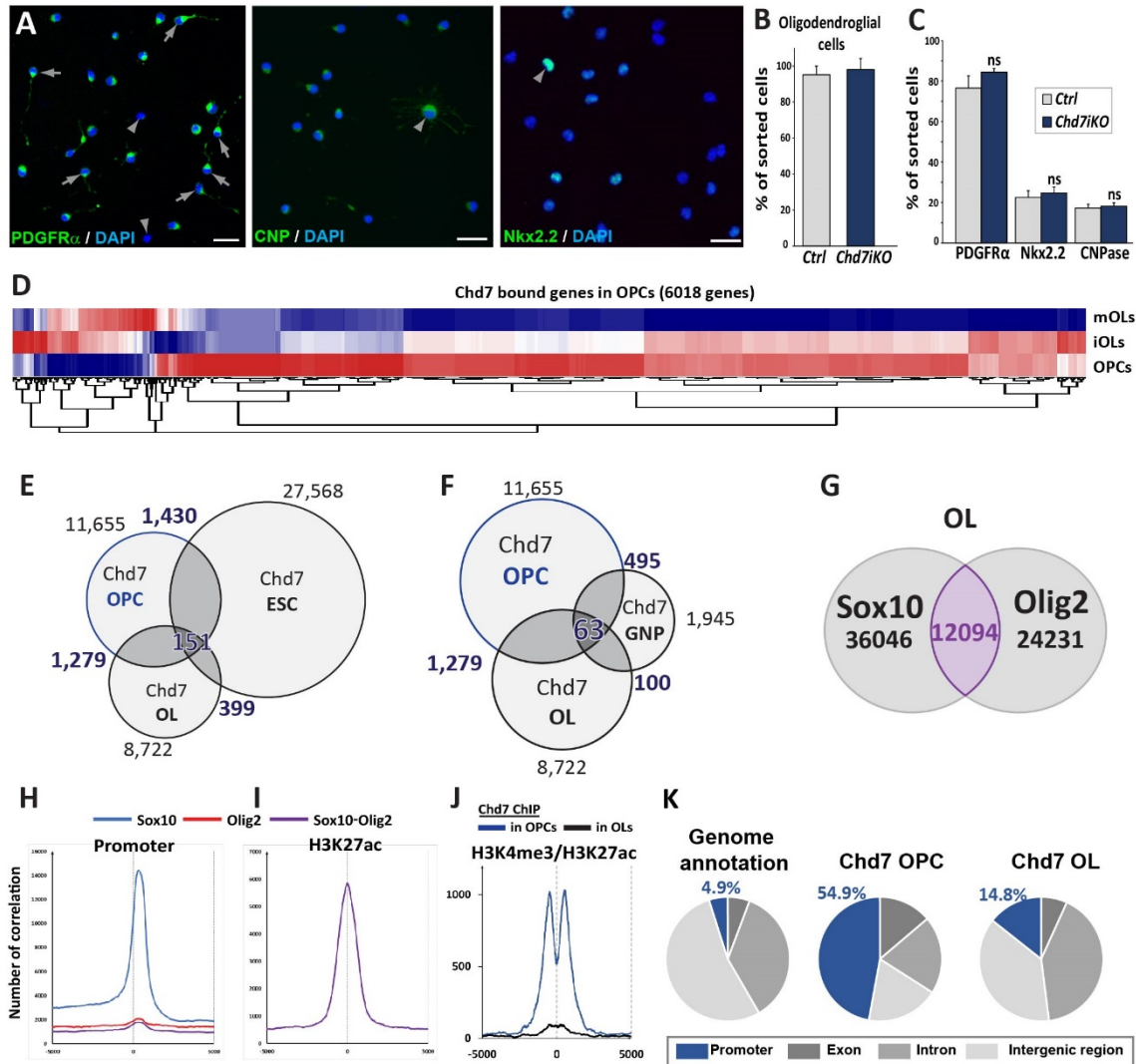


**Fig. S2. (related to Figure 1)**

A – Immunostaining showing PDGFR $\alpha$ , CNP and Nkx2.2 expression in MACS-sorted O4<sup>+</sup> cells of P7 mice. Scale bar: 10 $\mu$ m.

B – Quantification of PDGFR $\alpha$ <sup>+</sup>-CNP<sup>+</sup> cells as a percentage of total sorted cells (DAPI) from P7 *Ctrl* and *iKO* brains. Data are presented as mean  $\pm$  s.e.m. (n = 6 *Ctrl* and 7 *iKO*; P = 0.376, t = 0.92; two-tailed unpaired Student's t test).

C – Quantification of PDGFR $\alpha$ <sup>+</sup>, Nkx2.2<sup>+</sup> and CNP<sup>+</sup> cells as a percentage of total sorted cells (DAPI) from P7 *Ctrl* and *iKO* mice. Data are presented as mean  $\pm$  s.e.m. (PDGFR $\alpha$ <sup>+</sup>, n = 5 *Ctrl* and 3 *iKO*; P = 0.17, t = 1.56; Nkx2.2<sup>+</sup>, n=5 *Ctrl* and 4 *iKO*; P = 0.46, t = 0.78; CNP<sup>+</sup>, n = 5 *Ctrl* and 5 *iKO*; P = 0.58, t = 0.57; two-tailed unpaired Student's t test).

D – Heat maps of Chd7 bound gene expression levels in oligodendroglia according to Zhang et al., RNA-seq dataset (GSE52564).

E – Venn diagrams depicting the overlap of Chd7 binding sites in OPCs, OLs and ESCs.

F – Venn diagrams depicting the overlap of Chd7 binding sites in OPCs, OLs and GNPs.

G – Venn diagrams depicting the overlap between Sox10 and Olig2 binding sites in OLs.

H,I – Graph showing the number of correlation of Sox10 (blue), Olig2 (red) and Sox10-Olig2 (purple) peaks in OLs compared to the central position of promoter (G) and H3K27ac mark regions (H).

J – Graph showing the number of correlations of Chd7 peaks in OPCs (blue) and OLs (black) compared to the position in active histone marks H3K4me3/H3K27ac regions.

K – Region annotation of Chd7 binding sites in OPCs (middle) and OLs (right) compared to region representation in the genome (left).

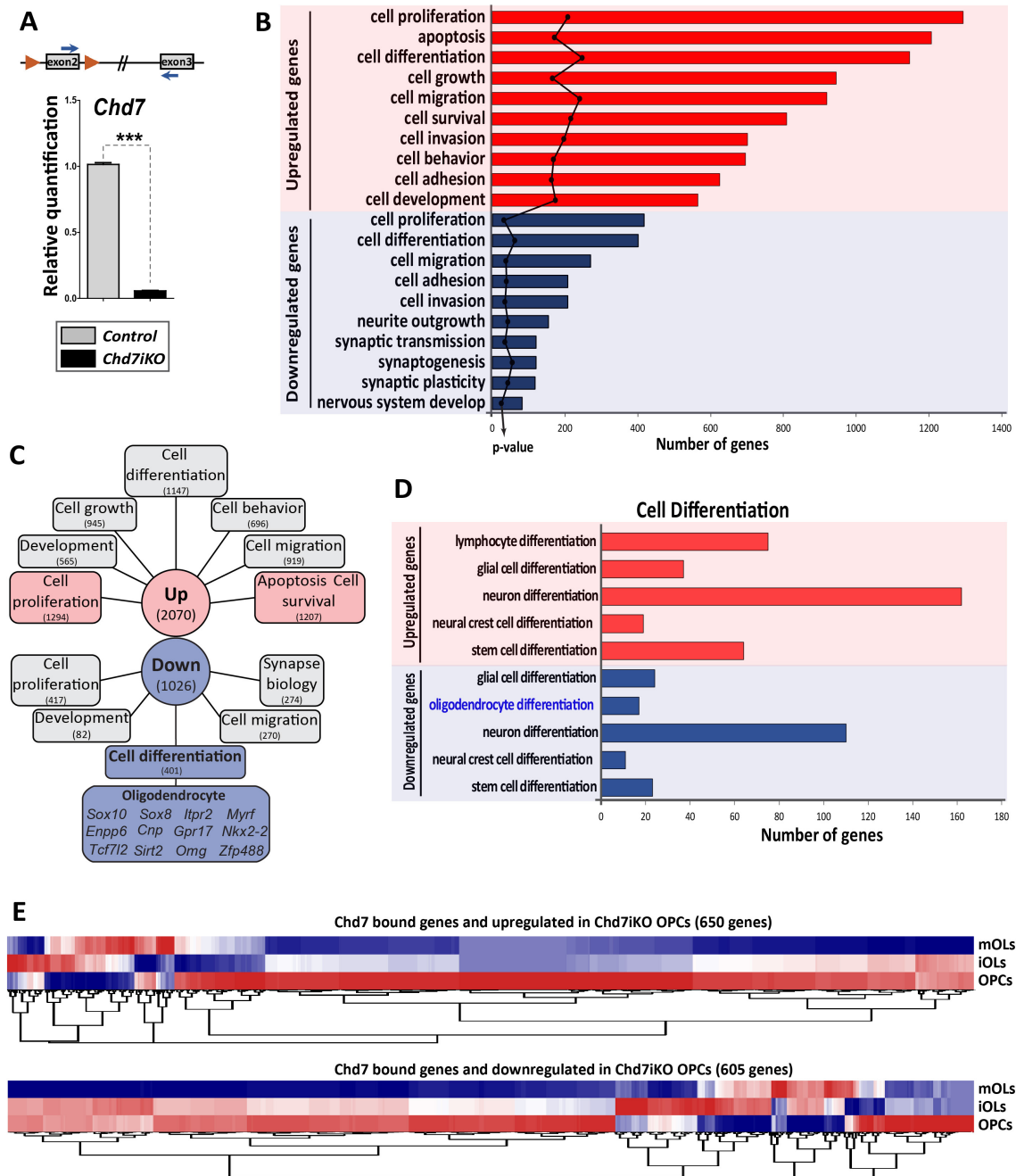


**Fig. S3. (related to Figure 2)**

A – Top, scheme of exons 2 and 3 of *Chd7* gene. Orange triangles represent *LoxP* sites, blue arrows represent primers used for RT-qPCR. Bottom, RT-qPCR analysis of *Chd7* deletion in P7 O4<sup>+</sup> cells of *Chd7iKO* (*iKO*) compared to *Crt1* mice. Normalization with  $\beta$ -actin. Data are presented as mean  $\pm$  s.e.m. ( $n = 7$  Controls and 7 *iKO*;  $P < 0.001$ ,  $t = 50.97$ ; two-tailed unpaired Student's  $t$  test). \* $P < 0.05$ , \*\* $P < 0.01$  and \*\*\* $P < 0.001$ .

B – Barplot showing the gene ontology (GO) analysis of the significantly upregulated (red) and downregulated (blue) genes in *control* and *iKO* mice. Line represents the Log(p-value).

C– Diagram representing the gene ontology (GO) analysis of the significantly upregulated and downregulated genes in *iKO* and *Ctrl* mice. The numbers indicate the number of genes of each category.

D – Barplot showing the gene ontology (GO) analysis of the significantly upregulated (red) and downregulated (blue) cell differentiation processes in *control* and *iKO* mice.

E – Heat maps of Chd7 bound gene expression levels in oligodendroglia according to Zhang et al., RNA-seq dataset (GSE52564).

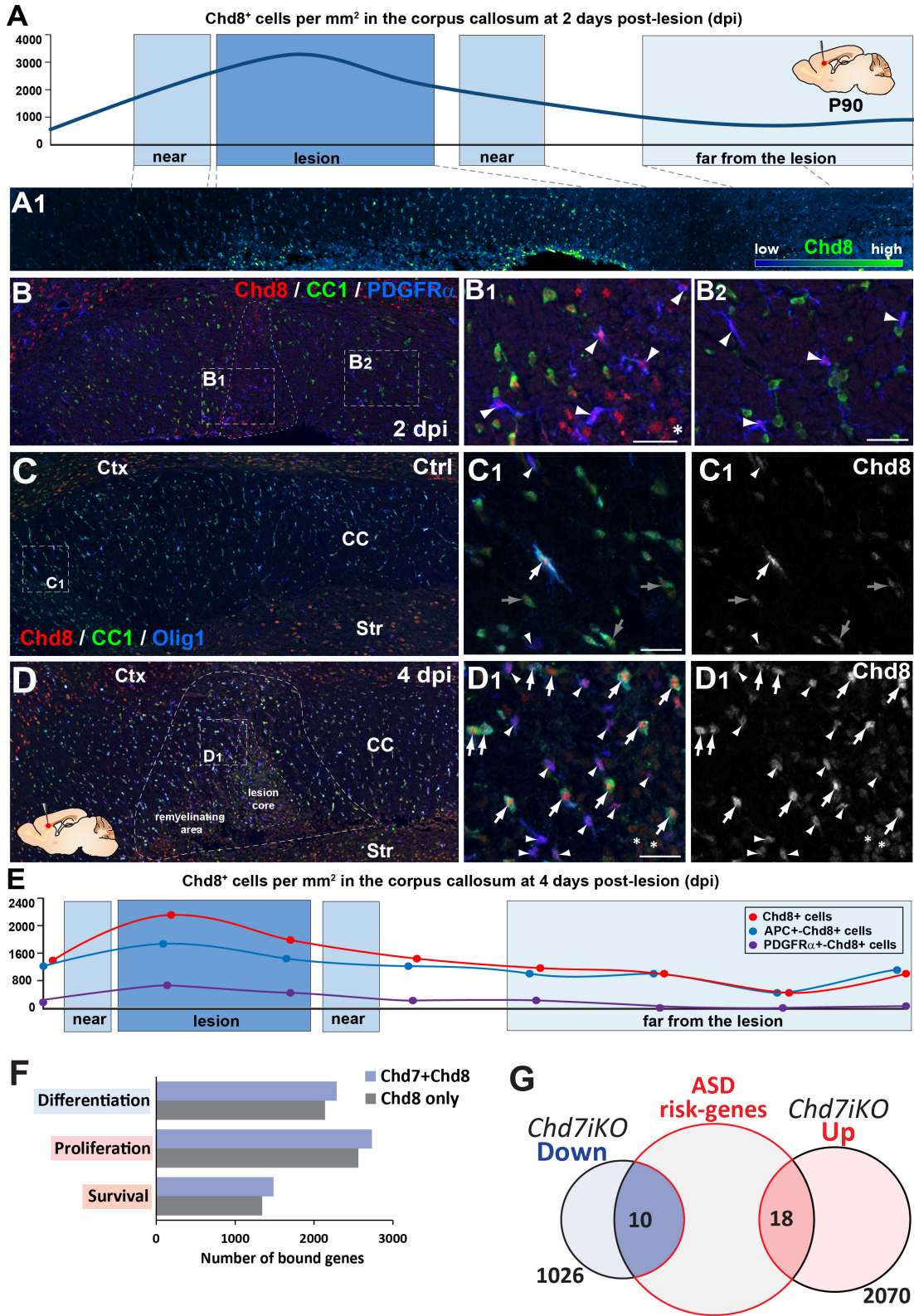


**Fig. S4. (related to Figure 3)**

A – Graphic representing Chd8<sup>+</sup> cells showing increased number of Chd8<sup>+</sup> cells in/around lesion. A1, Chd8 immunofluorescence levels presented in green-blue gradient color code showing high levels of Chd8 in cells in/around the lesion.

B – Immunofluorescence showing the lesion area at 2 dpi (dotted line) by the absence of CC1<sup>+</sup> OLs where PDGFR $\alpha$ <sup>+</sup>-OPCs express strong levels of Chd8. Comparison of Chd8 expression found in OPCs present at a distance from the lesion (B2) and OPCs inside lesions (B1). Arrow heads represent PDGFR $\alpha$ <sup>+</sup>-OPCs. Asterisk indicate Chd8 cells not expressing oligodendroglial markers, most likely corresponding to microglial/macrophage cells.

C – Immunofluorescence showing Chd8 expression in corpus callosum of control adult mouse. C1 is a higher magnification of the inset in C showing Chd8 expression in adult Olig1<sup>+</sup>-OPCs (arrows) and low Chd8 expression in CC1<sup>+</sup>-OLs (grey arrows)

D – Immunofluorescence showing the lesion area and remyelinating area at 4 dpi (dotted line) by the presence of iOLs (CC1<sup>high</sup>/Olig1<sup>-</sup>) where OPCs (Olig1<sup>+</sup> cells) and iOLs express strong levels of Chd8. D1 is a higher magnification of the inset in D, in remyelinating area. Arrows represent iOLs, arrow heads represent OPCs. Asterisk indicate Chd8 cells not expressing oligodendroglial markers, most likely corresponding to microglial/macrophage cells.

E – Graphic representing the density of Chd8<sup>high</sup> expressing cells in the corpus callosum at 4 dpi. Note that the lesion core devoid of OLs has been excluded from the representation. Ctx, cortex; Stri, striatum; CC, corpus callosum. Scale bar, 20 $\mu$ m.

F – Barplot representing the gene ontology (GO) analysis of the Chd7/Chd8- or Chd8-only bound genes.

G – Venn diagram depicting the overlap between ASD risk-genes and regulated genes in *Chd7iKO* OPCs.



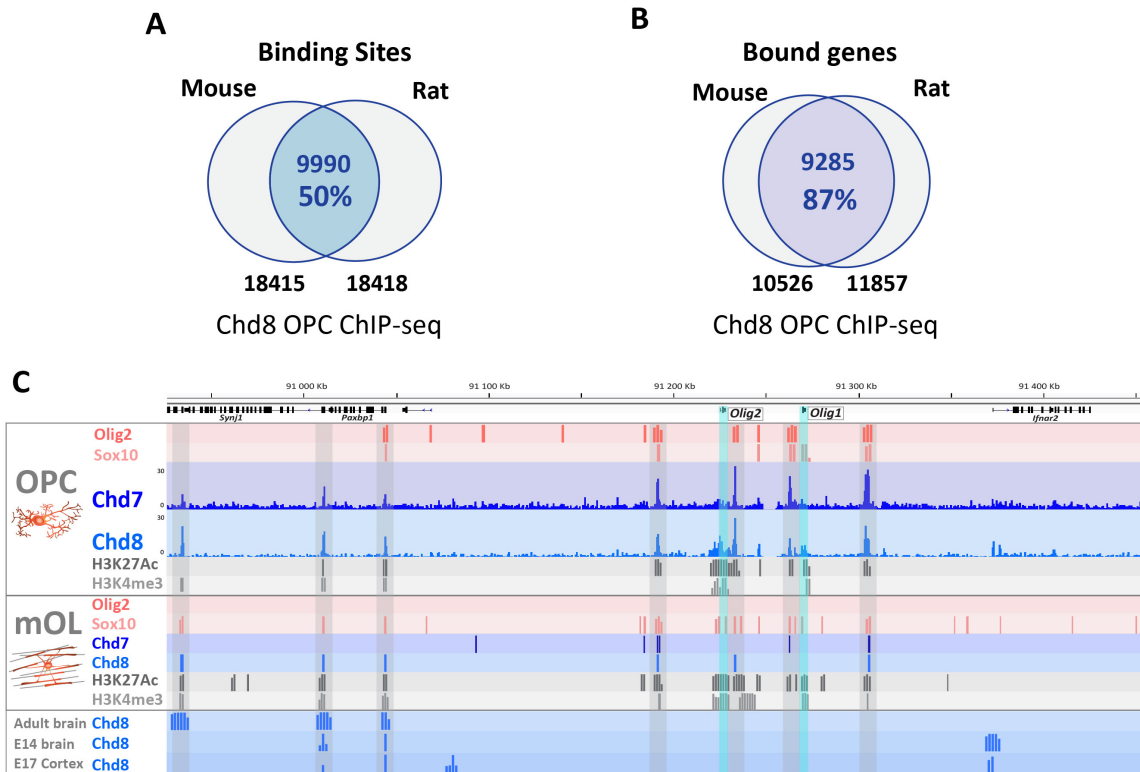


**Fig. S5. (related to Figure 3)**

A – Venn diagrams depicting the overlap of Chd8 binding sites found in MACS-sorted OPCs from P7 mice and cultured OPCs from neonatal rats (Zhao et al. Dev Cell, on-line).

B – Venn diagrams depicting the overlap of Chd8 bound genes found in MACS-sorted OPCs from P7 mice and cultured OPCs from neonatal rats (Zhao et al. Dev Cell, on-line), showing a large number of common genes.

C – Schematic representation from IGV genome browser of *Olig1* and *Olig2* integrating ChIP-seq data for main oligodendroglial TFs (Olig2 and Sox10), chromatin remodeling factors (Chd7, Chd8) and active epigenetic marks (H3K27ac and H3K4me3) in OPCs and OLs, together with Chd8 ChIP-data from embryo (E14.5) or adult brain (Katayama et al., Nature 2016) or E17.5 frontal or occipital cortex (GSE57369, Cotney et al., Nat. Commun. 2015).

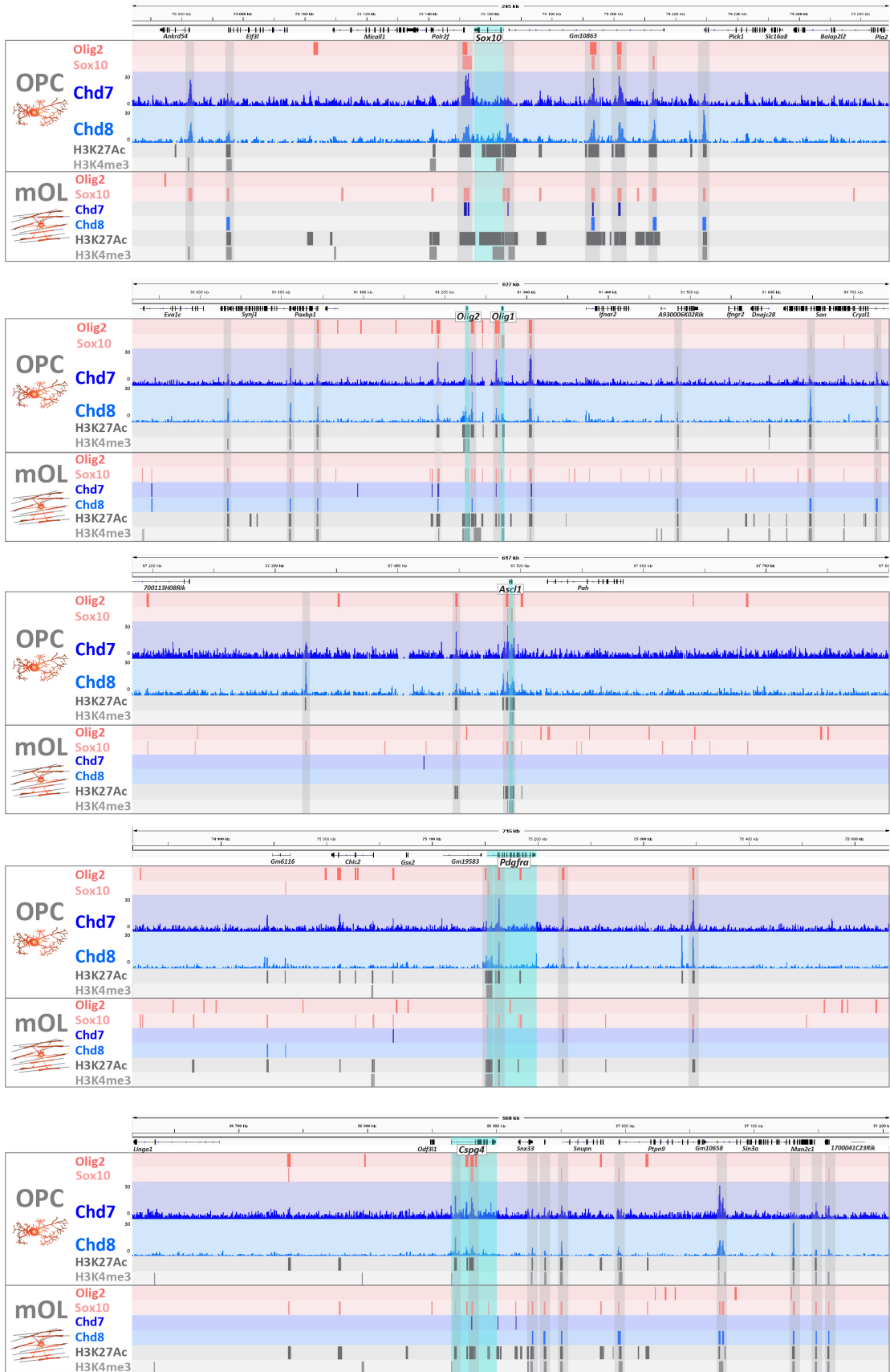


**Fig. S6. (related to Figure 3)**

Schematic representation from IGV genome browser of selected oligodendroglial regulators and OPC-marker genes (i.e. *Sox10*, *Olig2*, *Ascl1*, *Pdgfra*, *Cspg4*) integrating ChIP-seq data for main oligodendroglial TFs (*Olig2* and *Sox10*), chromatin remodeling factors (*Chd7*, *Chd8*) and active epigenetic marks (*H3K27ac* and *H3K4me3*) in OPCs and OLs.

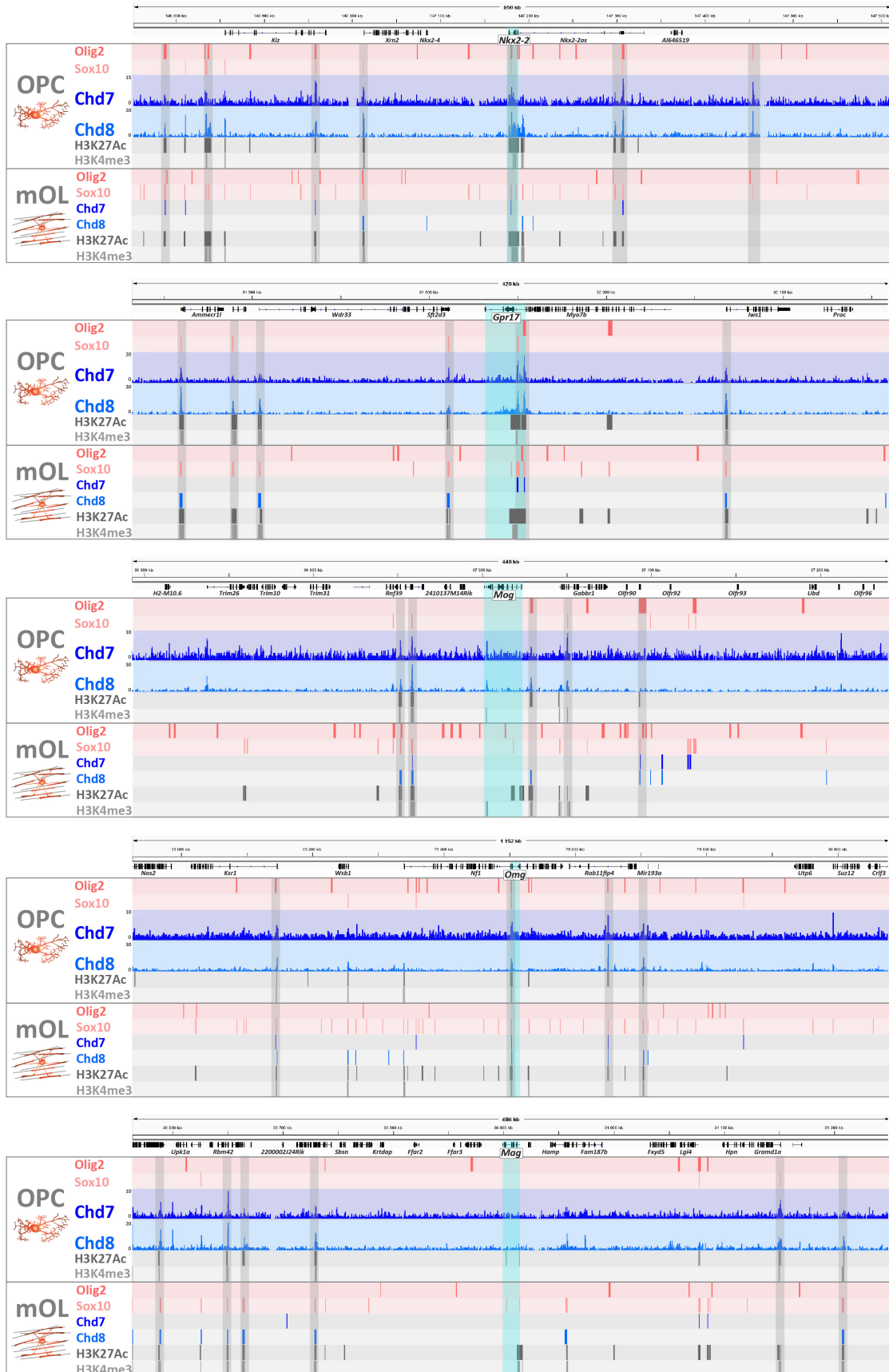


**Fig. S7. (related to Figure 3)**

Schematic representation from IGV genome browser of oligodendroglial regulators and myelin protein genes (i.e. *Nkx2-2*, *Gpr17*, *Mog*, *Omg*, *Mag*) integrating CHIP-seq data for main oligodendroglial TFs (Olig2 and Sox10), chromatin remodeling factors (Chd7, Chd8) and active epigenetic marks (H3K27ac and H3K4me3) in OPCs and OLS.

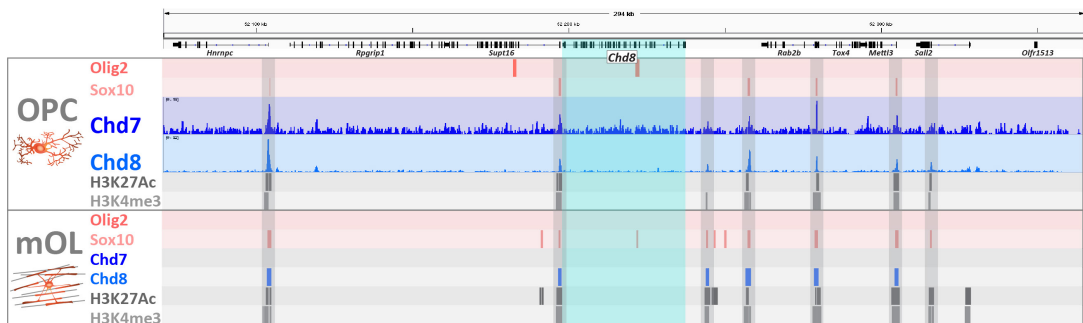
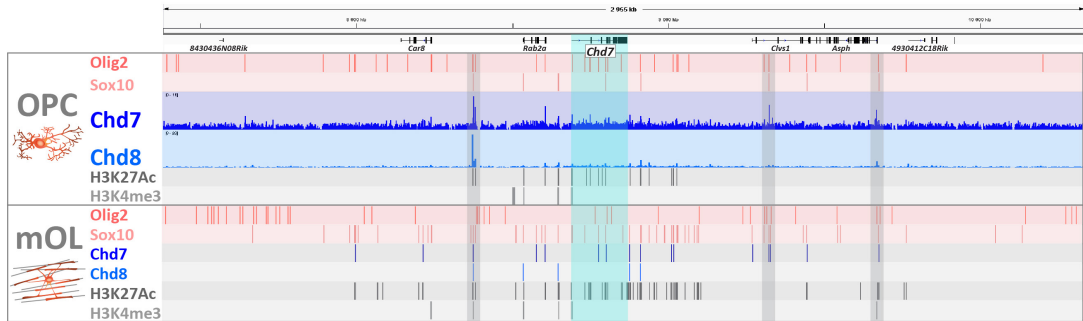
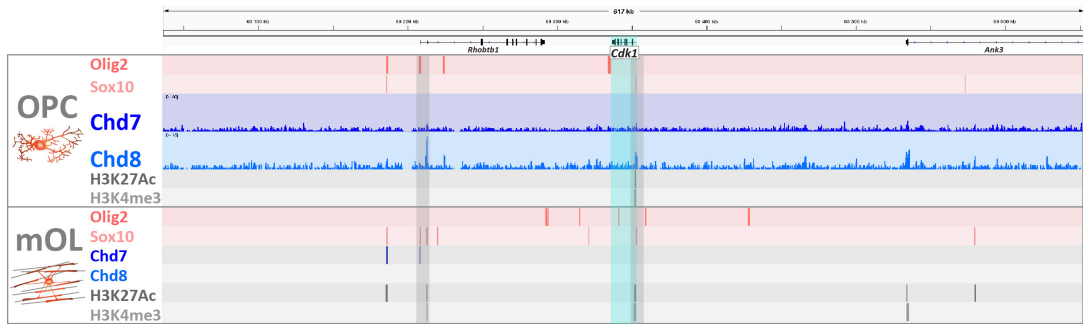
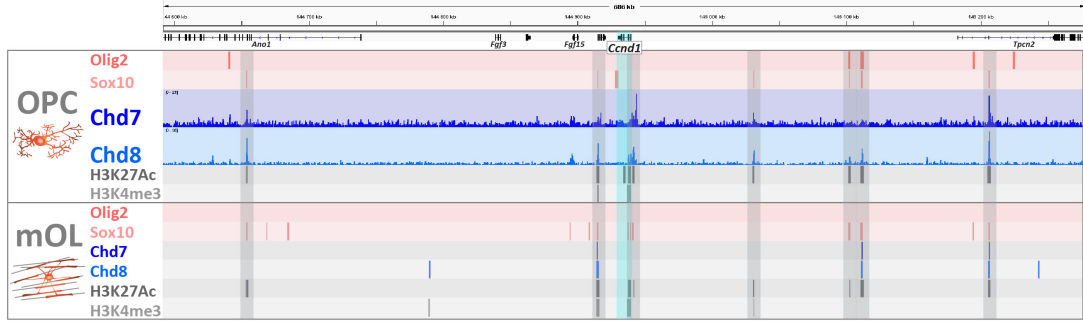
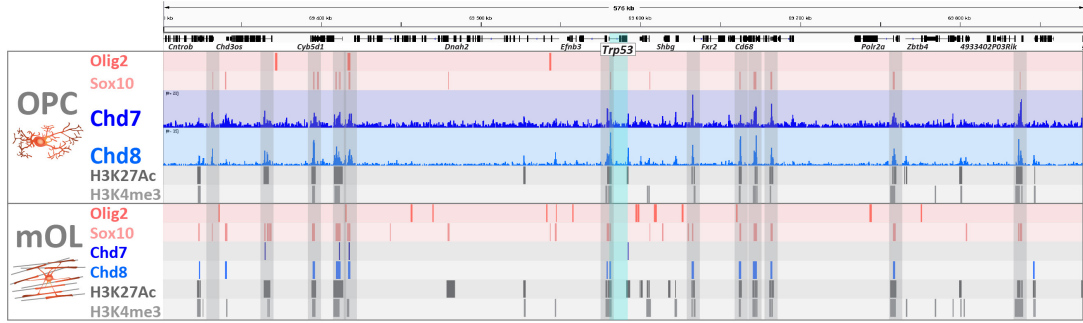


**Fig. S8. (related to Figure 3)**

Schematic representation from IGV genome browser of selected genes (i.e. *Trp53*, *Ccnd1*, *Cdk1*, *Chd7*, *Chd8*) integrating CHIP-seq data for main oligodendroglial TFs (Olig2 and Sox10), chromatin remodeling factors (Chd7, Chd8) and active epigenetic marks (H3K27ac and H3K4me3) in OPCs and OLs.

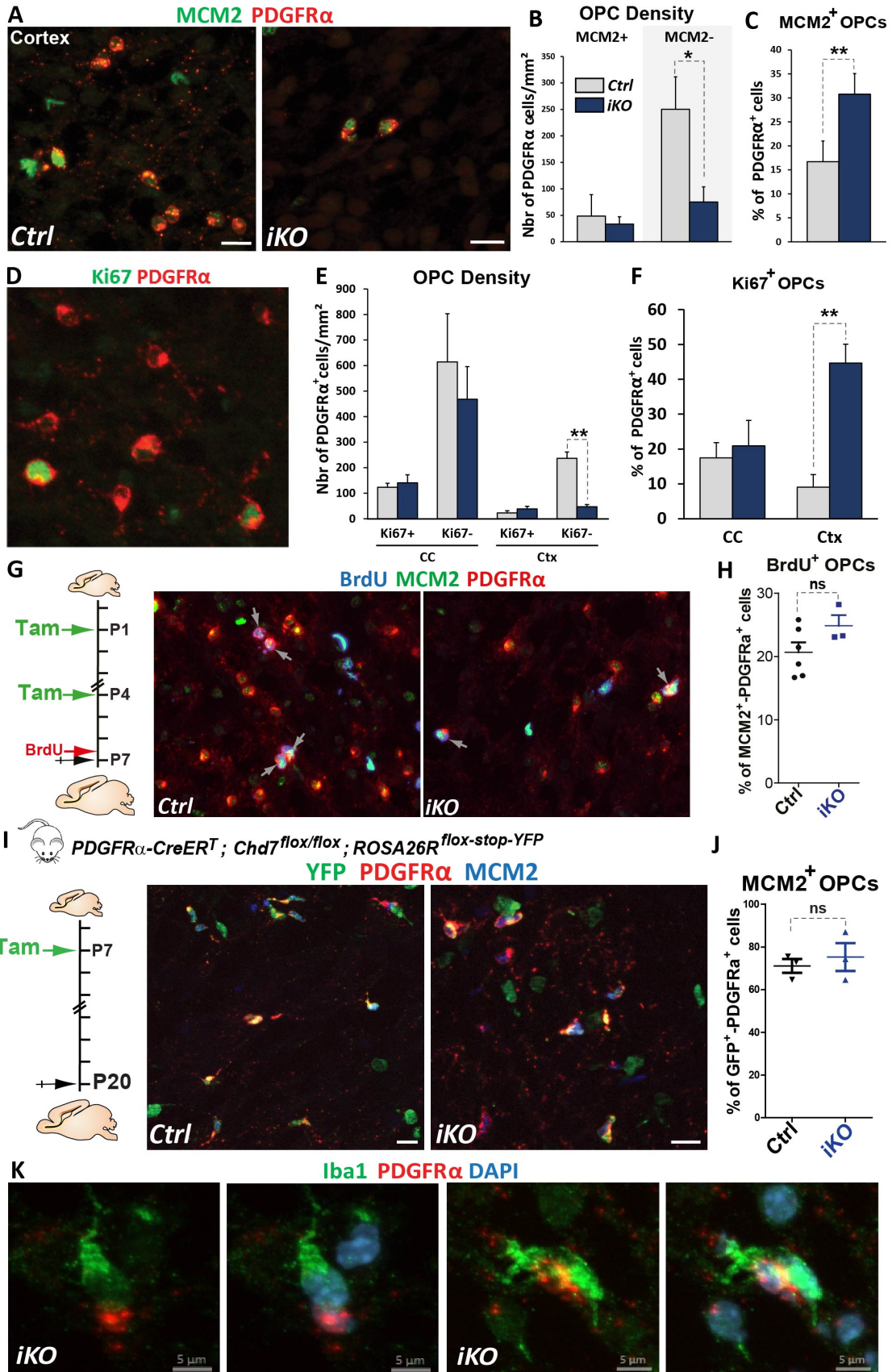




**Fig. S9. (related to Figure 4 & 5)**

A – Immunostaining of MCM2 and PDGFR $\alpha$  in the cortex of P7 *Ctrl* and *iKO* mice. Scale bar: 10  $\mu$ m.

B – Quantification of MCM2<sup>+</sup> and MCM2<sup>-</sup> OPCs (PDGFR $\alpha$ <sup>+</sup>) (nb/mm<sup>2</sup>) in the cortex of P7 *Ctrl* and *iKO* mice. Data are presented as mean  $\pm$  s.e.m. (MCM2<sup>+</sup>, n = 3 *Ctrl* and 3 *iKO*, P = 0.21, t = 1.51; MCM2<sup>-</sup>, n = 3 *Ctrl* and 3 *iKO*, P = 0.017, t = 3.96; two-tailed unpaired Student's t test).

C – Quantification of MCM2<sup>+</sup> OPCs as a percentage of total PDGFR $\alpha$ <sup>+</sup> cells in the cortex of P7 *Ctrl* and *iKO* mice. Data are presented as mean  $\pm$  s.e.m. (n = 3 *Ctrl* and 3 *iKO*, P = 0.003, t = 6.37; two-tailed unpaired Student's t test).

D – Immunostaining of Ki67 and PDGFR $\alpha$  in the corpus callosum of P7 mice. Scale bar: 10  $\mu$ m.

E – Quantification of Ki67<sup>+</sup> and Ki67<sup>-</sup> OPCs (PDGFR $\alpha$ <sup>+</sup>) (nb/mm<sup>2</sup>) in the corpus callosum (CC) and cortex (Ctx) of P7 *Ctrl* and *iKO* mice. Data are presented as mean  $\pm$  s.e.m. (CC, Ki67<sup>+</sup>, n = 3 *Ctrl* and 3 *iKO*, P = 0.445, t = 0.86; Ki67<sup>-</sup>, n = 3 *Ctrl* and 4 *iKO*, P = 0.271, t = 1.24; Ctx, Ki67<sup>+</sup>, n = 3 *Ctrl* and 3 *iKO*, P = 0.113, t = 2.02; Ki67<sup>-</sup>, n = 3 *Ctrl* and 3 *iKO*, P < 0.001, t = 12.60; two-tailed unpaired Student's t test).

F – Quantification of Ki67<sup>+</sup> OPCs as a percentage of total PDGFR $\alpha$ <sup>+</sup> cells in the corpus callosum (CC) and cortex (Ctx) of P7 *Ctrl* and *iKO* mice. Data are presented as mean  $\pm$  s.e.m. (CC, n = 3 *Ctrl* and 4 *iKO*, P = 0.50, t = 0.72; Ctx, n = 3 *Ctrl* and 3 *iKO*, P < 0.001, t = 9.48; two-tailed unpaired Student's t test).

G – Left, Diagram representing tamoxifen (Tam) administration to P1 and P4 *Ctrl* and *iKO* mice followed by BrdU injection 1 hour before perfusion at P7. Right, Immunostaining of MCM2, BrdU and PDGFR $\alpha$  in the corpus callosum of P7 *Ctrl* and *iKO* mice. Arrows show BrdU<sup>+</sup>-MCM2<sup>+</sup>-PDGFR $\alpha$ <sup>+</sup> cells. Scale bar: 10  $\mu$ m.

H – Quantification of BrdU<sup>+</sup> cells as a percentage of total MCM2<sup>+</sup>/PDGFR $\alpha$ <sup>+</sup> cells in the CC of P7 *Ctrl* and *iKO* mice. Data are presented as mean  $\pm$  s.e.m. (n = 6 *Ctrl* and 3 *iKO*, P = 0.14, t = 1.65; two-tailed unpaired Student's t test).

I – Left, Diagram representing tamoxifen (Tam) administration to P7 *Ctrl* and *iKO* YFP-reporter mice followed by analysis at P20. Right, Immunostaining of MCM2, GFP and PDGFR $\alpha$  in the corpus callosum of P20 *Ctrl* and *iKO* mice. Scale bar: 10  $\mu$ m.

J – Quantification of MCM2<sup>+</sup> cells as a percentage of total GFP<sup>+</sup>/PDGFR $\alpha$ <sup>+</sup> cells in the CC of P20 *Ctrl* and *iKO* mice. Data are presented as mean  $\pm$  s.e.m. (n = 3 *Ctrl* and 3 *iKO*, P = 0.6, t = 0.57; two-tailed unpaired Student's t test). \*P < 0.05, \*\*P < 0.01 and \*\*\*P < 0.001.

K – Immunostaining of Iba1 and PDGFR $\alpha$  in the cortex of P7 *Chd7cKO* mouse showing Iba1<sup>+</sup> microglia in close contact with PDGFR $\alpha$ <sup>+</sup> OPCs.

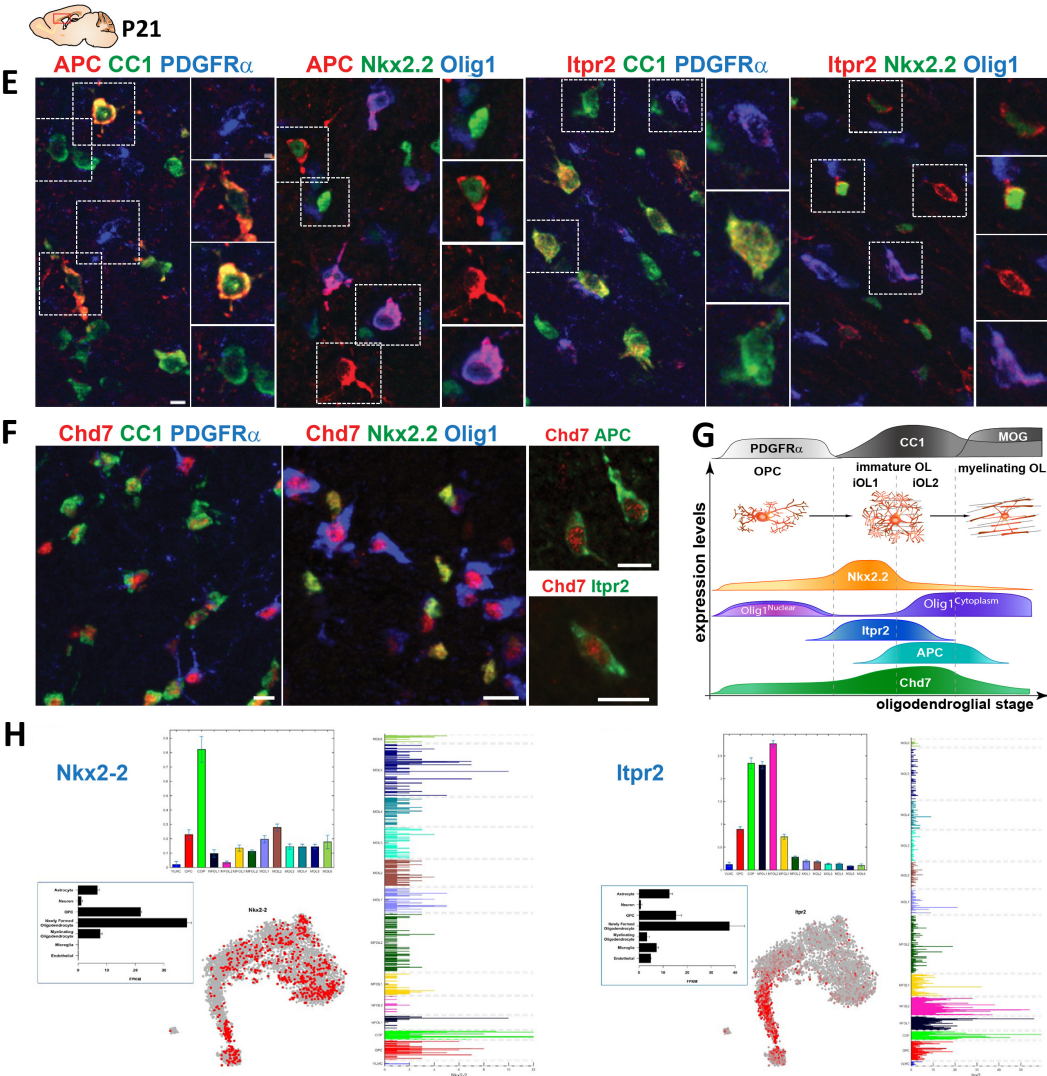
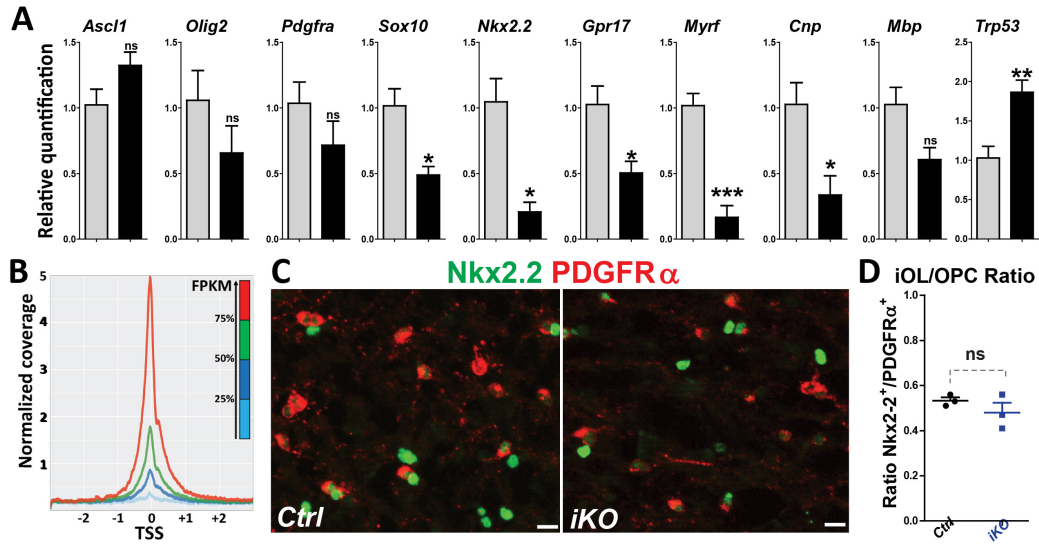


**Fig. S10. (related to Figure 6)**

A – RT-qPCR analysis of OL differentiation- and maturation-related genes in O4<sup>+</sup> cells isolated from P7 *Ctrl* and *Chd7iKO* (*iKO*) mice. Normalization with  $\beta$ -actin. Data are presented as mean  $\pm$  s.e.m. (n = 4 Controls and 4 *iKO*; *Ascl1*, P = 0.126, t = 1.83; *Olig2*, P = 0.266, t = 1.25; *PDGFR $\alpha$* , P = 0.251, t = 1.30; *Sox10*, P = 0.022, t = 3.61; *Nkx2.2*, P = 0.012, t = 3.825; *Gpr17*, P = 0.013, t = 3.29; *Myrf*, P < 0.001, t = 6.47; *Cnp*, P = 0.035, t = 3.13; *Mbp*, P = 0.059, t = 2.42; two-tailed unpaired Student's t test).

B – Graph showing the ATAC signal normalized coverage in the transcription start site (TSS) of genes differentially expressed in OPCs from the 25% of less expressed genes (blue) to the 25% most expressed genes (red).

C – Immunostaining of PDGFR $\alpha$  and Nkx2.2 in the corpus callosum of P7 *Ctrl* and *iKO* mice. Scale bar: 10  $\mu$ m.

D – Ratio between Nkx2.2<sup>+</sup> iOLs and PDGFR $\alpha$ <sup>+</sup> OPCs in the corpus callosum of P7 *Ctrl* and *iKO* mice. Data are presented as mean  $\pm$  s.e.m. (n = 3 *Ctrl* and 3 *iKO*, P = 0.31, t = 1.16; two-tailed unpaired Student's t test).

E – APC and *Itpr2* expression during OL differentiation: APC and *Itpr2* immunolabeling is compared with PDGFR $\alpha$ , *Olig1*, Nkx2.2 and CC1 expression in the corpus callosum of wild-type P21 mice. Scale bars: 10  $\mu$ m.

F – Immunostaining showing *Chd7* expression and co-labeling of PDGFR $\alpha$ , *Olig1*, Nkx2.2, CC1, APC and *Itpr2*. Scale bar: 10  $\mu$ m.

G – Scheme representing expression levels of different stage specific-OL differentiation markers.

H – RNA-seq expression data of Nkx2-2 and *Itpr2* transcripts from Zang & Barres 2014 ([http://web.stanford.edu/group/barres\\_lab/brain\\_rnaseq.html](http://web.stanford.edu/group/barres_lab/brain_rnaseq.html)) and Marques & Castelo-Branco 2016 (<http://linnarssonlab.org/oligodendrocytes/>) databases.

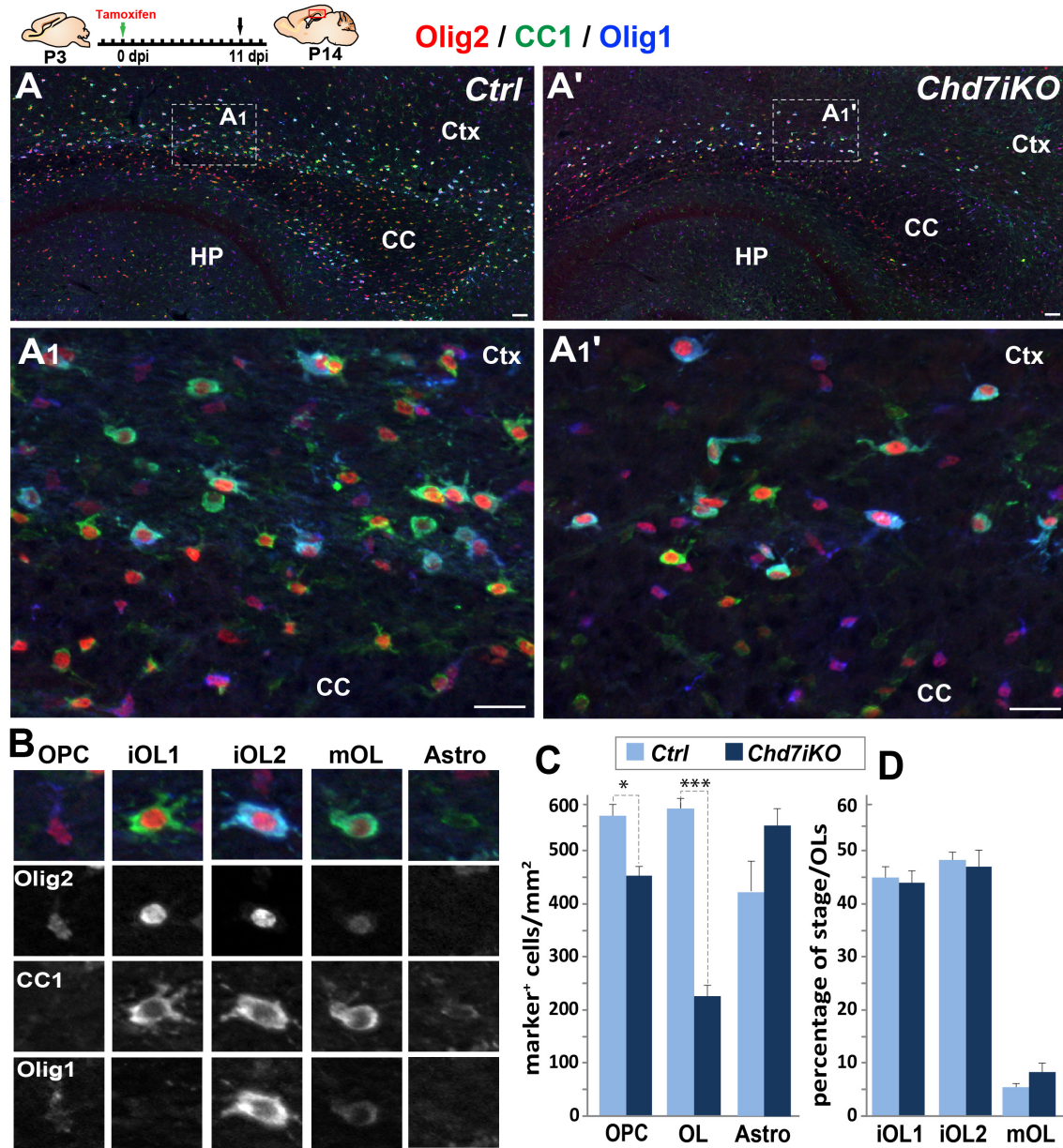


**Fig. S11. (related to Figure 6)**

A – Top, diagram of the Tamoxifen (Tam) administration at P3 followed by tissue collecting at P14. Bottom, immunostaining of Olig2, APC/CC1 and Olig1 in the corpus callosum of P14 *Ctrl* (A) and *Chd7iKO* (*cKO<sup>OPC</sup>*, A') mice. A2 and A2': High magnification of insets in A and A', respectively. Scale bar: 20  $\mu$ m.

B – Immunostaining of Olig2, APC/CC1 and Olig1 used to distinguish OL stages: OPCs (Olig1<sup>nuclear</sup>) iOL1 (CC1<sup>high</sup>-Olig1<sup>-</sup>), iOL2: (CC1<sup>high</sup>-Olig1<sup>cyto</sup>), mOLs(CC1<sup>+</sup>-Olig1<sup>cyto</sup>) and astrocytes (CC1<sup>low</sup>).

C - Quantification of OPCs ( $\text{Olig1}^{\text{nuclear}}$ ), OL ( $\text{CC1}^{\text{high}}$ ) and astrocytes ( $\text{CC1}^{\text{low}}$ ) cells ( $\text{nb}/\text{mm}^2$ ) in P14 *Ctrl* and *cKO* mice. Data are presented as mean  $\pm$  s.e.m.

D - Quantification of iOL1 ( $\text{CC1}^{\text{high}}\text{-Olig1}^-$ ), iOL2 ( $\text{CC1}^{\text{high}}\text{-Olig1}^{\text{cyto}}$ ) and mOLs ( $\text{CC1}^+\text{-Olig1}^{\text{cyto}}$ ) as a percentage of total  $\text{CC1}^+$  OL lineage cells in P14 *Ctrl* and *Chd7 cKO* mice. Data are presented as mean  $\pm$  s.e.m.

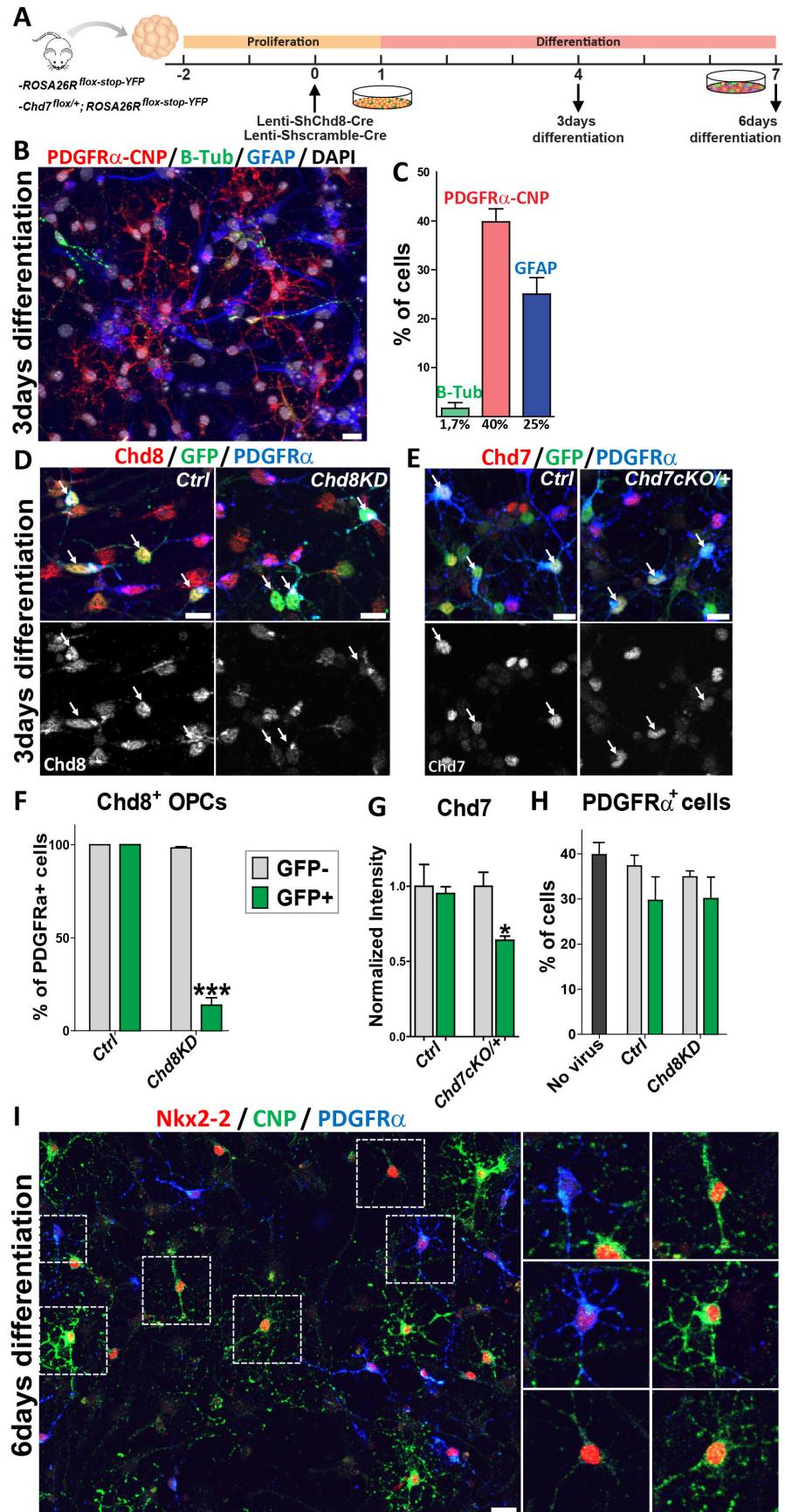


**Fig. S12. (related to Figure 7)**

A – Diagram representing NSCs proliferation and differentiation following infection by a lentivirus expressing Cre and a scramble shRNA or a shRNA against Chd8 and followed by fixation after 3 or 6 days of differentiation.

B – Immunostaining of PDGFR $\alpha$ -CNP,  $\beta$ -Tubulin and GFAP in WT cells after 3 days in differentiation medium. Scale bar: 10  $\mu$ m.

C – Quantification of  $\beta$ -Tubulin<sup>+</sup>, PDGFR $\alpha$ -CNP<sup>+</sup> and GFAP<sup>+</sup> cells as a percentage of total WT cells after 3 days in differentiation medium. Data are presented as mean  $\pm$  s.e.m.

D – Immunostaining of Chd8 and PDGFR $\alpha$  together with GFP in *Ctrl* (*ROSA26R<sup>stop-floxed-YFP</sup>* transduced with lentivirus expressing Cre and scramble shRNA) and *Chd8KD* (*ROSA26R<sup>stop-floxed-YFP</sup>* transduced with lentivirus expressing Cre and shRNA against Chd8) cells after 3 days in differentiation medium. Arrows represent PDGFR $\alpha$ <sup>+</sup>-GFP<sup>+</sup> OPCs. Scale bar: 10  $\mu$ m.

E – Immunostaining of Chd7 and PDGFR $\alpha$  together with GFP in *Ctrl* and *Chd7cKO/+* (*Chd7<sup>Flox/+</sup>; ROSA26R<sup>stop-floxed-YFP</sup>* transduced with lentivirus expressing Cre and scramble shRNA) cells after 3 days in differentiation medium. Arrows represent PDGFR $\alpha$ <sup>+</sup>-GFP<sup>+</sup> OPCs. Scale bar: 10  $\mu$ m.

F – Quantification of Chd8<sup>+</sup> OPCs as a percentage of total PDGFR $\alpha$ <sup>+</sup> cells in *Ctrl* and *Chd8KD* cells after 3 days in differentiation medium. Data are presented as mean  $\pm$  s.e.m. (n = 3; P < 0.001, t = 21.51; two-tailed unpaired Student's t test).

G – Quantification of normalized intensity of Chd7 staining in PDGFR $\alpha$ <sup>+</sup> cells in GFP<sup>+</sup> or GFP<sup>-</sup> cells in *Ctrl* and *Chd7cKO/+* conditions after 3 days in differentiation medium. Data are presented as mean  $\pm$  s.e.m.

(n = 3; P = 0.0215, t = 3,662; two-tailed unpaired Student's t test).

H – Quantification of PDGFR $\alpha$ <sup>+</sup>-GFP<sup>+</sup> cells as a percentage of total GFP<sup>+</sup> and GFP<sup>-</sup> cells after 3 days in differentiation medium in *WT*, *Ctrl*, *Chd8KD*, *Chd7cKO/+* and *Chd7cKO/+ ; Chd8KD* conditions. Data are presented as mean  $\pm$  s.e.m.

I – Immunostaining of Nkx2.2, CNP and PDGFR $\alpha$  in WT cells after 6 days in differentiation medium, showing Nkx2.2 *in vitro* expression during OPC differentiation. Scale bar: 10  $\mu$ m.

J – Immunostaining of Nkx2.2,  $\beta$ -Tubulin and PDGFR $\alpha$  in WT cells after 6 days in differentiation medium. Scale bar: 10  $\mu$ m. \*P < 0.05, \*\*P < 0.01 and \*\*\*P < 0.001.



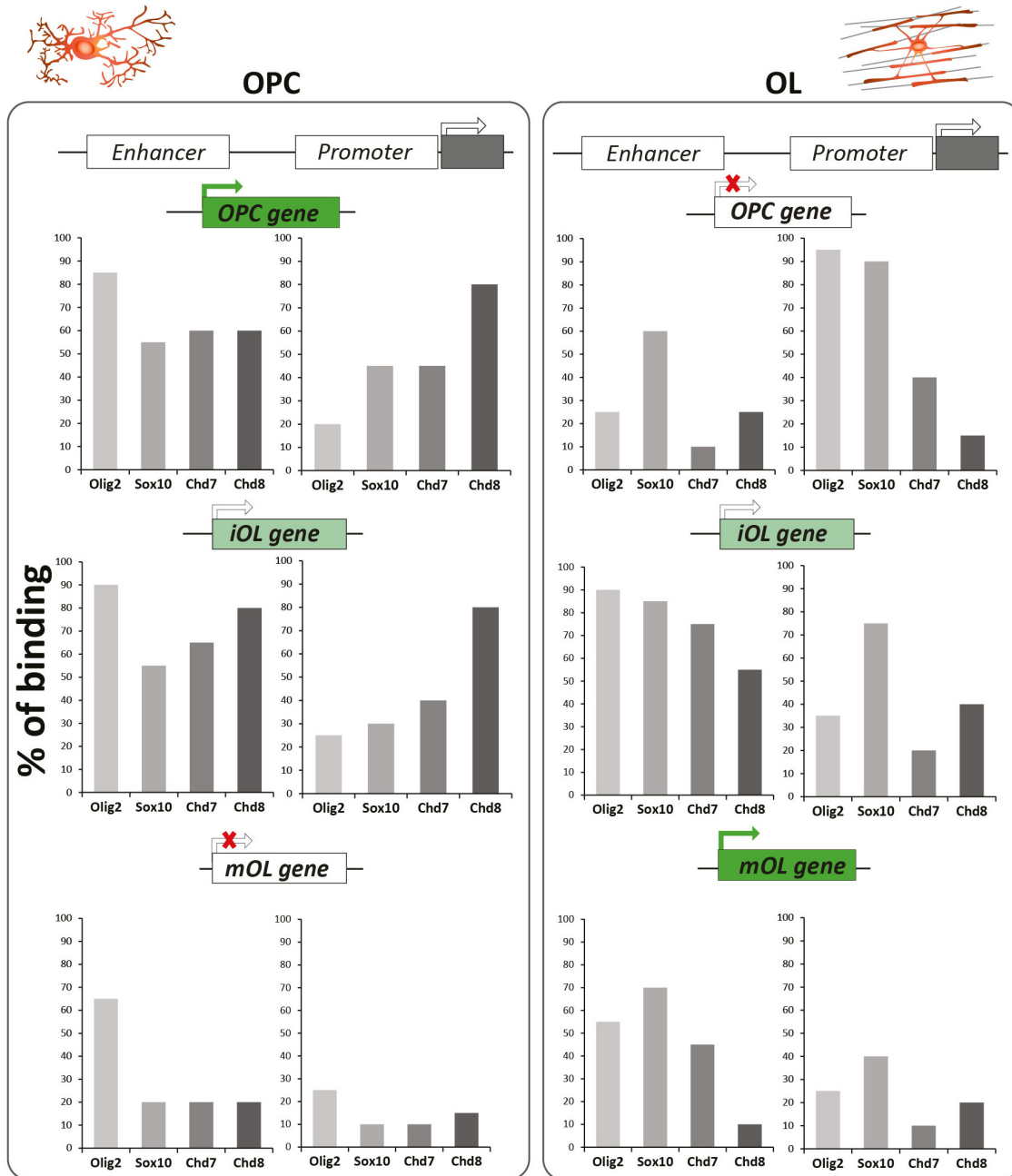


**Fig. S13. (related to Figure 8)**

Quantification of the percentage of binding of key transcription factors (Sox10, Olig2, Ascl1) and chromatin remodelers (Chd7, Chd8 and Brg1) in promoter and enhancer regions of each gene group (OPC, iOL and mOL) in OPCs and OLs. n=20 genes (list in Table S1).

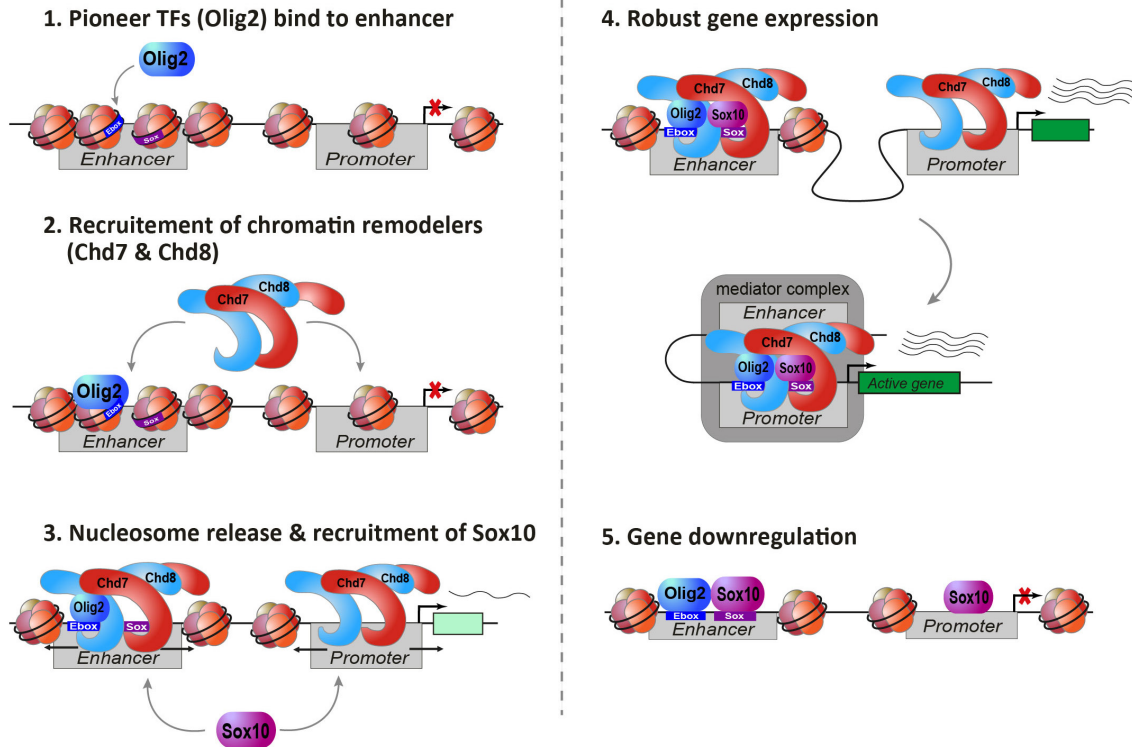


**Fig. S14. (related to Figure 8)**

Model of transcriptional regulation of oligodendroglia stage-specific gene. (1) Olig2 binds first to enhancers of ‘not yet expressed’ genes, in agreement with the pioneer factor function of Olig2. (2) Chd7 and Chd8 are then recruited by Olig2 in promoter and/or enhancer regions of these genes. (3) They slide nucleosomes to open chromatin, resulting in Sox10 binding. (4) Binding of Chd7, Chd8, Olig2 and Sox10 together with the recruitment of mediator complex stabilize the promoter-enhancer loop and enhance a strong gene expression. (5) Remarkably, downregulated genes are still bound by Olig2 and Sox10 in OLs.

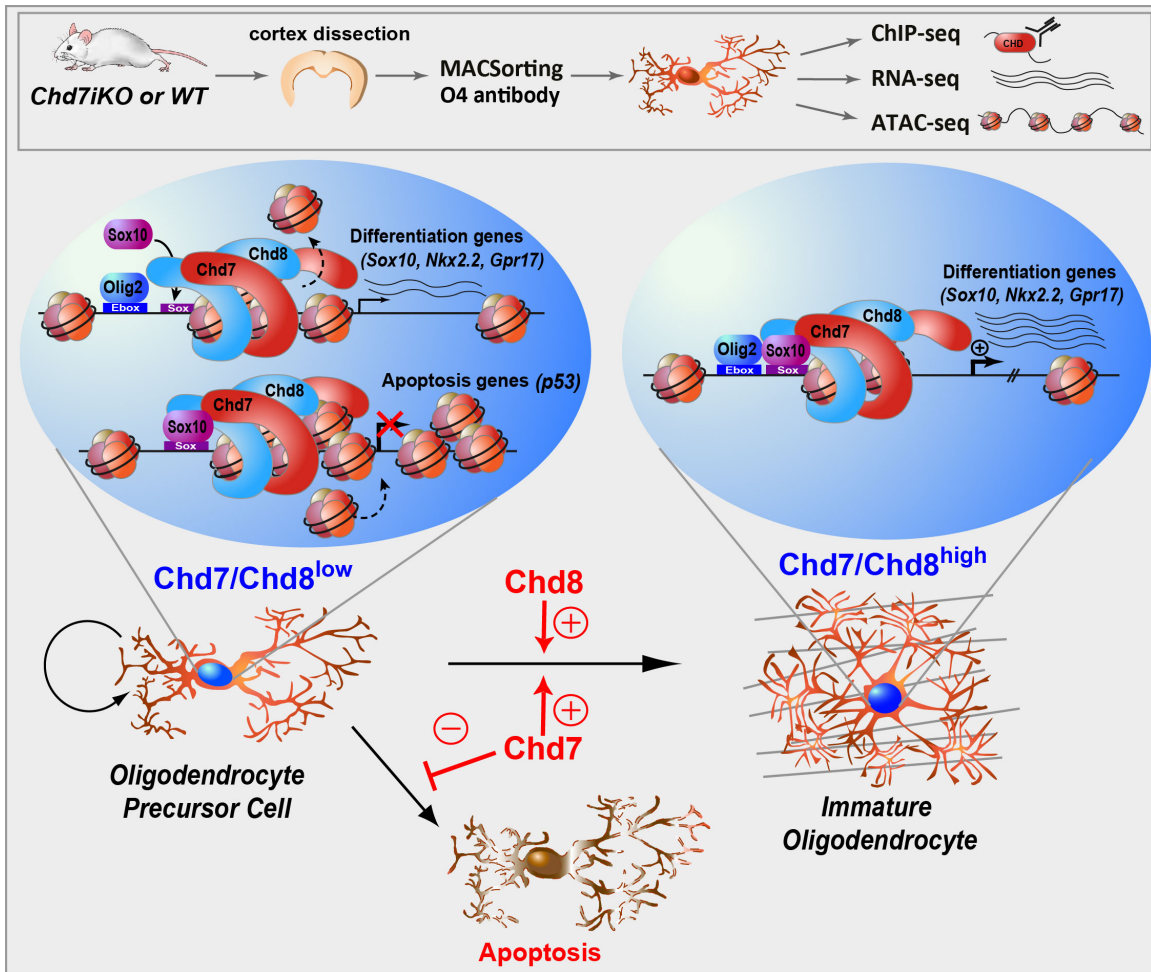


**Fig. S15. Graphical abstract**

- Genome-wide chromatin binding profile of Chd7 and Chd8 from *in vivo* OPCs
- Chd7 and Chd8 bind to the same promoter and enhancer regions of OPC differentiation-, proliferation- and survival-genes
- Chd7 induces OPC differentiation by chromatin-opening and gene activation of *Sox10*, *Nkx2.2*, *Gpr17*
- Chd7 promotes OPC survival by chromatin-closing and transcription repression of *p53*

OPC genes	iOL genes	mOL genes
Pdgfra	Gpr17	Omg
Cspg4	Itpr2	Apc
Ascl1	Zfp488	Mobp
Id2	Nkx2-2	Mag
Ptprz1	Sirt2	Nkx6-2
Serpine2	Myrf	Mog
Fabp7	Cnp	Ermn
Ednrb	Enpp6	Opalin
Sdc3	Plp1	Trf
Lhfpl3	Mbp	Car2
Ccnd1	Neu4	Mal
Ntm	Sox6	Gsn
Sox11	Traf4	Aspa
Zfp36l1	Slc1a1	Ndr1
Pcdh15	Frmd4a	Pdlim2
Kcnip3	Mpzl1	Sepp1
Matn4	Tns3	Cntn2
Slc1a2	Kank1	Glul
Tmem100	Col9a3	Grb14
Gria3	Tril	Phgdh

**Table S1.**

List of oligodendroglia stage-specific genes used for quantifying the binding of key transcription factors (Sox10, Olig2, Ascl1) and chromatin remodelers (Chd7, Chd8 and Brg1) to promoter and enhancer regions of each gene group (OPC, iOL and mOL) in OPCs and OLs.

<b>Gene</b>	<b>Forward</b>	<b>Reverse</b>	<b>Reference</b>
<b><i>β-actin</i></b>	TCCTAGCACCATGAAGATCAAGATC	CTGCTTGCTGATCCACATCTG	This paper
<b><i>Chd7</i></b>	CAGCAGCATCTGCATCATCT	GACCCAGGTGTCCAGAAGAG	This paper
<b><i>p53</i></b>	GGGGAGGAGCCAGGCCATCA	CCGCGCCATGGCCATCTACA	This paper
<b><i>Cnp1</i></b>	TCCACGAGTGCAAGACGCTATTCA	TGTAAGCATCAGCGGACACCATCT	This paper
<b><i>MBP</i></b>	CCAAGTTCACCCCTACTCCA	TAAGTCCCGTTTCCTGTTG	Finzsch et al., J Cell Biol., 2010
<b><i>Sox10</i></b>	CAGGTGTGGCTCTGCCACG	GTGTAGAGGGGCCGCTGGGA	Finzsch et al., J Cell Biol., 2010
<b><i>Nkx2.2</i></b>	TGGCCATGTACACGTTCTGA	CCGATGCTCAGGAGACGAAA	Shiimura et al., Int J Endocrinol., 2015
<b><i>Gpr17</i></b>	ACACAGTTGTCTGCCTGCAA	GCCGTAGTGGGTAGTTCTTG	Chen et al., Nat Neurosci., 2009
<b><i>Myrf</i></b>	CCTGTGTCCGTGGTACTGTG	TCACACAGGCGGTAGAAGTG	Hornig et al., PLoS Genet., 2013
<b><i>Olig2</i></b>	GAAGCAGATGACTGAGCCCGAG	CCCGTAGATCTCGCTCACCAG	Hornig et al., PLoS Genet., 2013
<b><i>Pdgfra</i></b>	ACAGAGACTGAGCGCTGACA	CTCGATGGTCTCGTCCTCTC	Hornig et al., PLoS Genet., 2013
<b><i>Ascl1</i></b>	ACTTGAAGTCTATGGCGGGTT	CCAGTTGGTAAAGTCCAGCAG	Voronova et al., PLoS One., 2011

**Table S2.**

List of mouse primers used for RTqPCR.

### **Dataset S1 (separate Excel file)**

A- Lists of genes bound by Chd7 in both OPCs and OLs, OPC-unique and OL-unique.

B- Lists of upregulated and downregulated genes bound by Chd7.

C- Lists of genes commonly or specifically bound by Chd7 and Chd8.

D-list of ASD-risk genes bound by Chd7 or Chd8.

E-Gene ontology

### **Dataset S2 (separate Excel file)**

Statistical analysis for each experiment with exact p-values, etc.

### **Supplemental references**

1. Kang SH, Fukaya M, Yang JK, Rothstein JD, & Bergles DE (2010) NG2+ CNS Glial Progenitors Remain Committed to the Oligodendrocyte Lineage in Postnatal Life and following Neurodegeneration. *Neuron* 68(4):668-681.
2. Hurd EA, Poucher HK, Cheng K, Raphael Y, & Martin DM (2010) The ATP-dependent chromatin remodeling enzyme CHD7 regulates pro-neural gene expression and neurogenesis in the inner ear. *Development* 137(18):3139-3150.
3. Srinivas S, *et al.* (2001) Cre reporter strains produced by targeted insertion of EYFP and ECFP into the ROSA26 locus. *BMC Dev Biol* 1:4.
4. Yu Y, *et al.* (2013) Olig2 Targets Chromatin Remodelers to Enhancers to Initiate Oligodendrocyte Differentiation. *Cell* 152(1-2):248-261.
5. He D, *et al.* (2017) lncRNA Functional Networks in Oligodendrocytes Reveal Stage-Specific Myelination Control by an lncOL1/Suz12 Complex in the CNS. *Neuron* 93(2):362-378.
6. Zhang Y, *et al.* (2014) An RNA-Sequencing Transcriptome and Splicing Database of Glia, Neurons, and Vascular Cells of the Cerebral Cortex. *The Journal of Neuroscience* 34(36):11929-11947.
7. Marques S, *et al.* (2016) Oligodendrocyte heterogeneity in the mouse juvenile and adult central nervous system. *Science* 352(6291):1326-1329.
8. Ernst J, *et al.* (2011) Mapping and analysis of chromatin state dynamics in nine human cell types. *Nature* 473(7345):43-49.